An AREVA and Stemens company

ANP-10262Q2NP Revision 000

April 2008

Response to Request for Additional Information – ANP-10262(P)



AREVA NP Inc.

ANP-10262Q2NP Revision 000

Response to Request for Additional Information – ANP-10262(P)

Copyright © 2008

AREVA NP Inc. All Rights Reserved

ANP-10262Q2NP Revision 000 Page i

Response to Request for Additional Information - ANP-10262(P)

Table of Contents

| Ques | <u>tion</u> |
|-------------|--|
| Question 1: | BYPASS BOILING METHODOLOGY |
| Question 2: | ADDITIONAL JUSTIFICATION FOR THE 5 PERCENT HOT CHANNEL OSCILLATION MAGNITUDE (HCOM) PENALTY |
| Question 3: | VALIDATION OF THE STEADY-STATE DRYOUT CORRELATIONS |
| Question 4: | JUSTIFICATION FOR THE 10 PERCENT DIVOM PENALTY FOR MELLLA+ |

This document contains a total of 42 pages.

Question 1: BYPASS BOILING METHODOLOGY

Please document the methodology to propagate errors induced by the presence of bypass boiling in the oscillation power range monitor (OPRM) channel calibration. In addition, provide the following information:

- What is the expected value of bypass voids at the C- and D- level detectors for operating limit thermal power (OLTP), Extended Power Uprates (EPU), and Maximum Extended Load Line Limit Analysis (MELLLA) domain (e.g., MELLLA+) in a representative reactor?
- 2. What is the expected calibration error induced by the presence of these bypass voids?
- For a representative reactor, provide a table with the value of all local power range monitor (LPRM) readings at a representative time. In addition, provide the LPRM-to-OPRM channel assignments for this reactor.
- 4. Using the above LPRM values, generate the response of each OPRM channel to an assumed core-wide 0.5 Hz oscillation. Use the following assumptions: (1) each LPRM oscillates with an amplitude proportional to their steady-state reading, (2) even though the oscillation is core-wide, assume a conservative value for the out-of-phase-mode phase lag for the D-level detector (e.g., 60 degrees).
- Repeat step 4 assuming that bypass boiling is present by applying the calibration error calculated in step 2.
- 6. Generate the P-A/A for the simulated OPRM signals in steps 4 and 5. Provide a table of the expected errors for each OPRM channel. To select a conservative value of the expected OPRM calibration error, assume that all of the OPRM channels that are allowed to be out of service by a representative technical specification requirement are the OPRM channels with lower error.

Response 1:

BWR core operation at high power and natural circulation may not result in sufficient core pressure drop to support upward bypass flow against the weight of a column of liquid water of the active core height. Boiling in the bypass is thus expected to balance the pressure drop, where direct bypass flow heating is provided by gamma radiation and neutron slowing down. Significant voiding in the bypass flow may occur at the upper elevation of the bypass channel where the level-D detectors are located, and to a lesser extent at level-C detectors. The LPRM detector signals are proportional to the thermal neutron flux, and thus the bypass voiding around a detector causes a local decrease in the thermal neutron flux and will result in a reduction of the signal-to-power ratio, i.e. the sensitivity of the detector is reduced resulting in a calibration error. The methodology to account for this calibration error is based on the following calculations:

a) Bypass flow and void faction distribution under natural circulation conditions using the core simulator MICROBURN-B2. A

- b) The detector calibration error is determined as function of the bypass void fraction by performing calculations at several exposure points using the lattice code CASMO4.
- c) Using the steps (a) and (b) above, the calibration error is determined at levels C and D detectors given the calculated bypass void distribution.
- d) The calibration error effect is integrated into the Enhanced Option III methodology according to the way the detector signals are utilized. Specifically,
 - For the purpose of oscillation magnitude setpoint comparison: An OPRM signal is made up of multiple LPRM detector signals where each LPRM signal may be at any level (A, B, C, or D). The combined signal is normalized and filtered before it is used for comparison with the relative amplitude setpoint, S_P. It has been found that the effect of the calibration error on the OPRM signal is negligible due to the normalization process, as will be demonstrated in the remainder of this response.
 - For the purpose of oscillation detection: The period-based detection algorithm (PBDA) utilizes OPRM signals to analyze their periodicity, not amplitude, and is therefore unaffected by calibration errors.
 - For the purpose of power level determination. An average power range monitor (APRM) signal is composed of several LPRMs taken at different elevations. There

are multiple APRM channels where their signals represent the average reactor fission power. For the Enhanced Option III solution, the single channel instability exclusion region is determined on the power/flow map based on measured flow and power, where the power information is obtained from the APRM response. Therefore, the calibration error of the upper elevation detectors will affect the APRM readings depending on the number and location of these upper level detectors and the relative power level at each of these detectors. The methodology is based on demonstration that the bypass voiding calibration error effect on APRM readings is significantly less than the conservative reduction of the exclusion region boundary power by 5% of rated. An example demonstration is provided as part of this response.

Expected Bypass Void Factions

The expected void fraction in the bypass for MELLLA operation at both the Original Licensed Thermal Power (OLTP) and EPU is the same since the corresponding core power of the MELLLA operating line at natural circulation is unchanged. Higher natural recirculation powers are obtained at natural circulation for MELLLA+. For both MELLLA and MELLLA+, no voiding was calculated at levels A and B. The maximum and average bypass void fraction at levels C and D are given below for different exposures points for the cases of running back along the MELLLA and MELLLA+ lines. The calculations show that the magnitude of bypass voiding is actually [] compared with MELLLA. The main reason for this observation is the higher power and bottom power peaking for MELLLA+, which leads to higher average core void fraction for the same flow rate, and this results in increased core pressure drop. The increased core pressure drop for MELLLA+ results in increasing bypass flow. [

Expected LPRM Calibration Errors due to Bypass Boiling

The calibration error relative to the signal is proportional to the void fraction in the bypass channel at the elevation where the detector is located. Other effects such as exposure of the bundles surrounding the detector were found to be small. The corresponding detector sensitivities to the above bypass voiding are given below.

LPRM Readings and OPRM Cell Assignments

The LPRM readings prior to oscillation inception, assuming no change in their sensitivity due to bypass boiling, are given in the table below:

| | | 이 관계 전 가슴 가슴 | leventet (11) e | 나는 이 사람이 사람이 나물이 물었다. | 이 이번 이 수 생각 |
|---------|--|--------------|-----------------|-----------------------|--------------|
| | LPRM | Level A | Level B | Level C | Level D |
| | 16-57 | 26.37 | 28.32 | 29.09 | 24.65 |
| | 24-57 | 64.03 | 53.17 | 44.13 | 32.08 |
| | 32-57 | 69.89 | 57.57 | 47.34 | 34.32 |
| | 40-57 | 42.74 | 40.17 | 38.17 | 30.47 |
| 1 | 08-49 | 37.78 | 39.3 | 36.5 | 27.99 |
| | 16-49 | 96.5 | 77.71 | 65.45 | 42.14 |
| | 24-49 | 76.16 | 62.74 | 56.2 | 48.9 |
| | 32-49 | 61.47 | 53.95 | 50.54 | 49.23 |
| | 40-49 | 92 | 72.65 | 64.02 | 45.11 |
| :- - | 48-49 | 87.81 | 70.76 | 56.86 | 35.73 |
| | 08-41 | 97.29 | 74.41 | 62.82 | 39.62 |
| | 16-41 | 79.99 | 67 | 59.89 | 41.65 |
| | 24-41 | 83.05 | 67.81 | 60.35 | 46.85 |
| - | 32-41 | 97.05 | 75.28 | 64.6 | 50.11 |
| • | 40-41 | 73.31 | 62.6 | 55.99 | 41.35 |
| 2 | 48-41 | 94.03 | 74.3 | 66.86 | 44.63 |
| | 56-41 | 45.32 | 41.9 | 40.38 | 30.93 |
| ¢ | 08-33 | 100.35 | 77.89 | 68.99 | 44.41 |
| | 16-33 | 92.09 | 75.62 | 68.3 | 48.75 |
| | 24-33 | 84.96 | 70.98 | 57.77 | 41.37 |
| 1 | 32-33 | 74.29 | 66.16 | 54.13 | 38.86 |
| ļ | 40-33 | 96.89 | 77.54 | 65.5 | 46.61 |
| - | 48-33 | 84.13 | 70.12 | 67.35 | 47.76 |
| | 56-33 | 75.56 | 60.62 | 52.02 | 34.95 |
| | 08-25 | 97.51 | 73.85 | 64.73 | 41.92 |
| | 16-25 | 80.06 | 66.78 | 59.86 | 41.82 |
| | 24-25 | 102.72 | 80.13 | 65.75 | 47.55 |
| | 32-25 | 99.58 | 78.48 | 65.45 | 48.01 |
| i. | 40-25 | 71.67 | 62.57 | 54.33 | 40.17 |
| ſ | 48-25 | 94.74 | 74.89 | 68.87 | 46.72 |
| | 56-25 | 69.53 | 56.18 | 48.15 | 32.89 |
| | 08-17 | 78.68 | 64.51 | 54.83 | 36.41 |
| | 16-17 | 91.52 | 74.9 | 66.8 | 45.41 |
| ÷ | 이 아이 | | to pay de pri | | |

| Response to Request for Add | ditional Informa | tion – ANP-10 | 0262(P) | | ANP-10262Q2NP Revision 000 Page 6 |
|-----------------------------|------------------|---------------|---------|---------|---|
| LPR | M Level A | Level B | Level C | Level D | |
| 24-17 | 7 75.77 | 62.92 | 56.31 | 51.1 | |
| 32-13 | 7 71.94 | 61.07 | 54.63 | 52.01 | |
| 40-17 | 7 91.4 | 72.36 | 65.36 | 48.06 | |
| 48-1 | 7 97.39 | 77.76 | 66.32 | 42.03 | |
| 56-1 | 7 26.78 | 29.05 | 30.16 | 24.94 | |
| 16-09 | 9 77.8 | 63.62 | 53.44 | 36.28 | |
| 24-09 | 9 89.89 | 68.81 | 58.4 | 41.34 | |
| 32-09 | 9 93.78 | 70.8 | 60.1 | 43.51 | |
| 40-09 | 9 93.19 | 71.79 | 59.09 | 39.26 | |
| 48-09 | 9 37.2 | 38.68 | 35.97 | 27.95 | |

The LPRM-to-OPRM assignments are given below:

| | | | | | for | | | | | | | | | | | |
|--|--|--|--|--|-----|--|--|--|--|--|--|--|--|--|--|--|
| | | | | | | | | | | | | | | | | |
| | | | | | | | | | | | | | | | | |
| | | | | | | | | | | | | | | | | |
| | | | | | | | | | | | | | | | | |
| | | | | | | | | | | | | | | | | |

| Cell ID# | LPRM #1 | LPRM #2 | LPRM #3 | LPRM #4 |
|----------|---------|---------|---------|---------|
| | 16-57B | 24-57C | 24-49C | 16-49B |
| 2 | 24-57C | 32-57D | 32-49D | 24-49C |
| 3 | 32-57D | 40-57A | 40-49A | 32-49D |
| 4 | 08-49A | 16-49B | 16-41D | 08-41C |
| 5 | 16-49B | 24-49C | 24-41A | 16-41D |
| 6 | 24-49C | 32-49D | 32-41B | 24-41A |
| 7 | 32-49D | 40-49A | 40-41C | 32-41B |
| 8 | 40-49A | 48-49B | 48-41D | 40-41C |
| 9 | 08-41C | 16-41D | 16-33D | 08-33C |
| 10 | 16-41D | 24-41A | 24-33A | 16-33D |
| 11 | 24-41A | 32-41B | 32-33B | 24-33A |
| 12 | 32-41B | 40-41C | 40-33C | 32-33B |
| 13 | 40-41C | 48-41D | 48-33D | 40-33C |
| . 14 | 48-41D | 56-41A | 56-33A | 48-33D |
| 15 | 08-33C | 16-33D | 16-25B | 08-25A |
| 16 | 16-33D | 24-33A | 24-25C | 16-25B |
| 17 | 24-33A | 32-33B | 32-25D | 24-25C |
| 18 | 32-33B | 40-33C | 40-25A | 32-25D |
| 19 | 40-33C | 48-33D | 48-25B | 40-25A |
| 20 | 48-33D | 56-33A | 56-25C | 48-25B |
| 21 | 08-25A | 16-25B | 16-17B | 08-17A |
| 22 | 16-25B | 24-25C | 24-17C | 16-17B |
| 23 | 24-25C | 32-25D | 32-17D | 24-17C |
| 24 | 32-25D | 40-25A | 40-17A | 32-17D |
| 25 | 40-25A | 48-25B | 48-17B | 40-17A |
| 26 | 48-25B | 56-25C | 56-17C | 48-17B |
| 27 | 16-17B | 24-17C | 24-09A | 16-09D |
| 28 | 24-17C | 32-17D | 32-09B | 24-09A |
| 29 | 32-17D | 40-17A | 40-09C | 32-09B |
| 30 | 40-17A | 48-17B | 48-09D | 40-09C |

Table 1-1 LPRM Detector to OPRM Cell Assignments for Channel 1

| Cell ID# | LPRM #1 | LPRM #2 | LPRM #3 | LPRM #4 |
|----------|---------|---------|---------|---------|
| 1 | 16-57C | 24-57A | 24-49D | 16-49D |
| 2 | 24-57A | 32-57A | 32-49B | 24-49D |
| 3 | 32-57A | 40-57C | 40-49B | 32-49B |
| 4 | 08-49B | 16-49D | 16-41A | 08-41A |
| 5 | 16-49D | 24-49D | 24-41C | 16-41A |
| 6 | 24-49D | 32-49B | 32-41C | 24-41C |
| 7 | 32-49B | 40-49B | 40-41A | 32-41C |
| 8 | 40-49B | 48-49D | 48-41A | 40-41A |
| 9 | 08-41A | 16-41A | 16-33B | 08-33D |
| 10 | 16-41A | 24-41C | 24-33B | 16-33B |
| 11 | 24-41C | 32-41C | 32-33D | 24-33B |
| 12 | 32-41C | 40-41A | 40-33D | 32-33D |
| 13 | 40-41A | 48-41A | 48-33B | 40-33D |
| 14 | 48-41A | 56-41C | 56-33B | 48-33B |
| 15 | 08-33D | 16-33B | 16-25C | 08-25C |
| 16 | 16-33B | 24-33B | 24-25A | 16-25C |
| 17 | 24-33B | 32-33D | 32-25A | 24-25A |
| 18 | 32-33D | 40-33D | 40-25C | 32-25A |
| 19 | 40-33D | 48-33B | 48-25C | 40-25C |
| 20 | 48-33B | 56-33B | 56-25A | 48-25C |
| 21 | 08-25C | 16-25C | 16-17D | 08-17B |
| 22 | 16-25C | 24-25A | 24-17D | 16-17D |
| 23 | 24-25A | 32-25A | 32-17B | 24-17D |
| 24 | 32-25A | 40-25C | 40-17B | 32-17B |
| 25 | 40-25C | 48-25C | 48-17D | 40-17B |
| 26 | 48-25C | 56-25A | 56-17D | 48-17D |
| 27 | 16-17D | 24-17D | 24-09C | 16-09A |
| 28 | 24-17D | 32-17B | 32-09C | 24-09C |
| 29 | 32-17B | 40-17B | 40-09A | 32-09C |
| 30 | 40-17B | 48-17D | 48-09A | 40-09A |

Table 1-2 LPRM Detector to OPRM Cell Assignments for Channel 2

| Cell ID# | LPRM #1 | LPRM #2 | LPRM #3 | LPRM #4 |
|----------|---------|---------|---------|---------|
| 1 | 16-57D | 24-57B | 24-49A | 16-49A |
| 2 | 24-57B | 32-57B | 32-49C | 24-49A |
| 3 | 32-57B | 40-57D | 40-49C | 32-49C |
| 4 | 08-49C | 16-49A | 16-41B | 08-41B |
| 5 | 16-49A | 24-49A | 24-41D | 16-41B |
| 6 | 24-49A | 32-49C | 32-41D | 24-41D |
| 7 | 32-49C | 40-49C | 40-41B | 32-41D |
| 8 | 40-49C | 48-49A | 48-41B | 40-41B |
| 9 | 08-41B | 16-41B | 16-33C | 08-33A |
| 10 | 16-41B | 24-41D | 24-33C | 16-33C |
| 11 | 24-41D | 32-41D | 32-33A | 24-33C |
| 12 | 32-41D | 40-41B | 40-33A | 32-33A |
| 13 | 40-41B | 48-41B | 48-33C | 40-33A |
| 14 | 48-41B | 56-41D | 56-33C | 48-33C |
| 15 | 08-33A | 16-33C | 16-25D | 08-25D |
| 16 | 16-33C | 24-33C | 24-25B | 16-25D |
| 17 | 24-33C | 32-33A | 32-25B | 24-25B |
| 18 | 32-33A | 40-33A | 40-25D | 32-25B |
| 19 | 40-33A | 48-33C | 48-25D | 40-25D |
| 20 | 48-33C | 56-33C | 56-25B | 48-25D |
| 21 | 08-25D | 16-25D | 16-17A | 08-17C |
| 22 | 16-25D | 24-25B | 24-17A | 16-17A |
| 23 | 24-25B | 32-25B | 32-17C | 24-17A |
| 24 | 32-25B | 40-25D | 40-17C | 32-17C |
| 25 | 40-25D | 48-25D | 48-17A | 40-17C |
| 26 | 48-25D | 56-25B | 56-17A | 48-17A |
| 27 | 16-17A | 24-17A | 24-09D | 16-09B |
| 28 | 24-17A | 32-17C | 32-09D | 24-09D |
| 29 | 32-17C | 40-17C | 40-09B | 32-09D |
| 30 | 40-17C | 48-17A | 48-09B | 40-09B |

Table 1-3 LPRM Detector to OPRM Cell Assignments for Channel 3

| | | | | genergi elegi inglar degi ogenergi 1999 - Alexie geteringen elegi er Arren deserviteri beter metering |
|----------|---------|---------|---------|---|
| Cell ID# | LPRM #1 | LPRM #2 | LPRM #3 | LPRM #4 |
| 1 | 16-57A | 24-57D | 24-49B | 16-49C |
| 2 | 24-57D | 32-57C | 32-49A | 24-49B |
| 3 | 32-57C | 40-57B | 40-49D | 32-49A |
| 4 | 08-49D | 16-49C | 16-41C | 08-41D |
| 5 | 16-49C | 24-49B | 24-41B | 16-41C |
| 6 | 24-49B | 32-49A | 32-41A | 24-41B |
| 7 | 32-49A | 40-49D | 40-41D | 32-41A |
| 8 | 40-49D | 48-49C | 48-41C | 40-41D |
| 9 | 08-41D | 16-41C | 16-33A | 08-33B |
| 10 | 16-41C | 24-41B | 24-33D | 16-33A |
| 11 | 24-41B | 32-41A | 32-33C | 24-33D |
| 12 | 32-41A | 40-41D | 40-33B | 32-33C |
| 13 | 40-41D | 48-41C | 48-33A | 40-33B |
| 14 | 48-41C | 56-41B | 56-33D | 48-33A |
| 15 | 08-33B | 16-33A | 16-25A | 08-25B |
| 16 | 16-33A | 24-33D | 24-25D | 16-25A |
| 17 | 24-33D | 32-33C | 32-25C | 24-25D |
| 18 | 32-33C | 40-33B | 40-25B | 32-25C |
| 19 | 40-33B | 48-33A | 48-25A | 40-25B |
| 20 | 48-33A | 56-33D | 56-25D | 48-25A |
| 21 | 08-25B | 16-25A | 16-17C | 08-17D |
| 22 | 16-25A | 24-25D | 24-17B | 16-17C |
| 23 | 24-25D | 32-25C | 32-17A | 24-17B |
| 24 | 32-25C | 40-25B | 40-17D | 32-17A |
| 25 | 40-25B | 48-25A | 48-17C | 40-17D |
| 26 | 48-25A | 56-25D | 56-17B | 48-17C |
| 27 | 16-17C | 24-17B | 24-09B | 16-09C |
| 28 | 24-17B | 32-17A | 32-09A | 24-09B |
| 29 | 32-17A | 40-17D | 40-09D | 32-09A |
| 30 | 40-17D | 48-17C | 48-09C | 40-09D |

Table 1-4 LPRM Detector to OPRM Cell Assignments for Channel 4

Assessment of Impact of Bypass Boiling on OPRM Signals

The requested signal is constructed for each detector using

$$LPRM(t) = LPRM(0) \cdot \zeta_{i} \cdot (1 + 0.1 \sin(2\pi \cdot f \cdot t - \theta_{i}))$$

Where

 θ_{l}

f

LPRM(t) Time dependent LPRM signal.

LPRM(0) Initial value of the LPRM signal.

 ζ_1 LPRM sensitivity factor due to bypass boiling corresponding to the detector level.

LPRM axial phase shift relative to level A. This will be set to 20 degrees for the B level, 40 degrees for the C level, and 60 degrees for the D level LPRMs.

Oscillation frequency, set equal to 0.5 Hz.

The generated OPRM signals with and without the effect of bypass boiling are calculated and compared for two sets of detector sensitivity reductions. In the first set, the levels C and D detector sensitivities are reduced to 95% and 90% respectively, which bounds the case specific examples determined above. In the second set, the levels C and D detector sensitivities are reduced to 90% and 80% respectively. The second set is provided to demonstrate the extreme insensitivity of the bypass boiling on the OPRM relative signals.

The percentage change in OPRM sensitivities for the first set (C level sensitivity = 95%, D level sensitivity = 90%) is given in the table below for all the OPRMs arranged in four trip channels.

ANP-10262Q2NP Revision 000 Page 13

The percentage change in OPRM sensitivities for the second set (C level sensitivity = 90%, D level sensitivity = 80%) is given in the table below for all the OPRMs arranged in four trip channels:

The corresponding statistics for the change in sensitivity is shown graphically in Figures 1-1 and 1-2 for the first and second set respectively. It is clear that there is a trend to [] not

[], sensitivity of most OPRM signals due to the improved signal coherence when the contribution of the upper level detectors with []. The few OPRMs where the sensitivity is slightly [

The OPRM detector sensitivities as function of the oscillation magnitude are displayed in Figures 1-3 and 1-4 for the two calculation sets respectively. These figures show that there is a majority of OPRMs with large absolute signal value (lower noise-to-signal ratio) where the sensitivity is either [______] by the bypass voiding. In this way, it is concluded that the OPRM relative signal for the purpose of comparison with the amplitude setpoint [______] possibility of some detectors being out-ofservice.

First Principle Interpretation of the Results

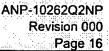
1

The effect of bypass boiling on the relative OPRM signal, for which numerical results are presented above, can be interpreted analytically. [

ANP-10262Q2NP Revision 000 Page 15

្ប៉ា

ľ



Effect of Bypass Boiling on APRM Calibration

An example of the effect of bypass boiling on the APRM signals is presented here. Actual APRM detector assignments into four channels have been used. A worst case results scenario was also assessed that assumed that the maximum allowable number of LPRM detectors to be out-of-service are entirely A and B level detectors which are not affected by bypass voiding. Even in this case, the largest effect on APRM sensitivity is [1] as shown in the table below.

j .

This corresponds to [] of rated power which is well within the 5% or rated conservative bias imposed by the Enhanced Option III solution on the computed channel exclusion region.

| _ | | | | | 4 4 4 4 7 1 3 3 4 4 5 1 | | | | |
|---|-------|---------------|-------------------|--|--|--|--|--|---|
| | esp | onse | to Request | for Additiona | al informatio | $n = ANP \cdot 10$ | 202(17) | <u></u> | Page 18 |
| - | 1212 | 12 12 12 12 h | | | at the farmer with the | ALCO 401 | 100/01 | | D 40 |
| | | | . ist state state | | and the second | and the second | ana an ing ing ing ing ing ing ing ing ing in | | |
| | 200 C | | | and the second se | | (1) A. | and the second second | a state of a second state of the | |
| | 1.1.1 | | | | | 1. 1. 15 (5) (5) | (1) A. 2 A. (1) A. | and the second | Revision 000 |
| | | | | | 4. 4 | in the special second | and the second second | - 「「「「「「」」」 「「」」 「」」 「」」 「」」 「」」 「」」 「」」 | The Company of the Araba |
| | | | | at a second second | | (1) (2) (2) (2) (2) (2) | and the second | · · · · · · · · · · · · · · · · · · · | 2. State of the |
| | | | | and a state of the | | · · · · · · · · · · · · · · · · · · · | | | THE FULLENCE IN |
| | | | | 1 | | | · · · · | and the second | |
| | | | | | | | · · · · · | | 4110 4000000000 |
| | | | | | | | | | |

Figure 1-1 Histogram of the Relative Change in the OPRM signals for 10% D level and 5% C level LPRM Signal Reduction

| nation - | nation - ANP-10262 | nation – ANP-10262(P) |
|----------|--------------------|-----------------------|

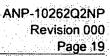


Figure 1-2 Histogram of the Relative Change in the OPRM signals for 20% D level and 10% C level LPRM Signal Reduction

| a si Casila | | · · · | | ANP- | 10262Q2NP |
|----------------|-------------|-----------|--|---|--------------|
| | | | | ₹_tracket | Revision 000 |
| Incoponio | c to reque. | | | | Page 20 |
| <u></u> | | | | | |
| • | | | | en an an an de Beern. D' an de personale est | |

5.

z (zzó)

Figure 1-3 Relative Change in the OPRM signals Versus Absolute Oscillation Magnitude for 10% D level and 5% C level LPRM Signal Reduction

ANP-10262Q2NP Revision 000 Page 21

Figure 1-4 Relative Change in the OPRM signals Versus Absolute Oscillation Magnitude for 20% D level and 10% C level LPRM Signal Reduction

(2.1)

Response to Request for Additional Information – ANP-10262(P)

Question 2: ADDITIONAL JUSTIFICATION FOR THE 5 PERCENT HOT CHANNEL OSCILLATION MAGNITUDE (HCOM) PENALTY

Please provide an expansion of Section 1.2 of TR ANP-10262(P) with a summary of the approved HCOM methodology (NEDO-32465-A). Provide a clear definition of what HCOM is, including the effect that higher decay ratios could have on the delta-critical power ratio (CPR) because of the delay on reactor shutdown after scram initiation.

Figure 3-6 of TR ANP-10262(P) shows that a biasing factor of 1.3 in the HCOM decay ratio (DR) probability distribution results in an amplitude setpoint change from 1.10 to 1.095 (i.e., 0.5 percent). Please describe how this result translates to a 5 percent HCOM penalty.

Note: the PBDA algorithm will trip the reactor when the DR becomes greater than 1.0. Under MELLLA+ conditions, a two-pump trip followed by the associated subcooling transient will result in a final DR significantly larger than under OLTP conditions, but the PBDA will scram the reactor at an earlier time (i.e., when the DR is approximately 1.0). With this argument in mind, please justify why a biasing factor of 1.3 conservatively represents the DR values that could be expected under MELLLA+ conditions at the time of scram (not the final DR).

Response 2:

HCOM is an acronym for "Hot Channel Oscillation Magnitude" where the hot channel is not necessarily the bundle with the highest power but more appropriately the one with the largest power swing so that its transient CPR is the limiting response of the core. The oscillation magnitude refers to the relative bundle power, and is defined as the peak bundle power (P) minus the preceding minimum bundle power (M) for a given oscillation cycle divided by the average power (A) over that oscillation period. Thus, HCOM = (P-M)/A.

The HCOM methodology refers to the analysis of the relationship between the hot channel oscillation magnitude (HCOM) and the trip amplitude setpoint S_P . The amplitude setpoint, S_P , is defined as the peak-to-average ratio of the OPRM signal at which a trip command is issued by the trip channel containing this OPRM. The HCOM analysis results in a few tabulated data pairs (normally 3 pairs) of HCOM versus S_P . Although not necessarily linear by definition, the relationship between S_P and HCOM obtained from actual analysis is almost exactly linear. Thus,

 $S_{p} = 1 + \xi \times HCOM$

where ξ is constant. Notice that the fractional part of S_P (not S_P itself) is proportional to HCOM because of their respective definitions. The HCOM analysis is effectively reduced to the methodology for determining the constant proportionality parameter, ξ .

In the idealized case where the detector response is measuring the power of a single bundle and the scram occurs immediately upon reaching the amplitude setpoint, the proportionality parameter $\xi = 0.5$ is obtained. However, the real system includes a plurality of OPRM detectors where each is made up of several LPRM detectors at different elevations, and each LPRM detector is mainly driven by the nearest four bundles instead of a single bundle. This reduces the proportionality parameter to $\xi \approx 0.3$ (exact value is plant-specific).

It is clear from Equation (2.1) that modification of the analysis assumptions in order to account for different stability conditions would alter the value of the parameter ξ . A reduction of ξ by 5% results in a reduction of the fractional part of the setpoint, $S_p - 1$, by the same 5% in order to protect the same HCOM. Equivalently, an existing analysis with the associated value of ξ unchanged can be used with a penalty of 5% applied to the HCOM value itself, with the same effect on the amplitude setpoint reduction.

The actual oscillation suppression due to the reactor scram lags the trip signal issued upon reaching the amplitude setpoint. Thus, the relationship between HCOM and S_P depends on the particular organization of the LPRM detector assignments to OPRM cells, and is also affected by the possibility of detectors out-of-service. The Detect & Suppress methodology as described in the topical report (NEDO-32465-A) requires a plant-specific statistical methodology for calculating a tabulated relationship between HCOM and S_P. This plant-specific HCOM methodology is described briefly below.

The HCOM statistical methodology applies a Monte Carlo technique to sample many cases to obtain the conservative 95% probability with 95% confidence value of the hot channel oscillation magnitude HCOM at the time of oscillation suppression for a given amplitude setpoint Sp. To characterize an oscillation for each case, the oscillation decay ratio (or more appropriately growth ratio) and the oscillation period are sampled from probability distributions shown in

(2.2)

Response to Request for Additional Information - ANP-10262(P)

Figures (4.4) and (4.5) of NEDO-32465-A, and the first oscillation peak that exceeds the amplitude setpoint is positioned randomly such that the setpoint is anywhere between that peak and the preceding one. In the worst case, a signal peak is very slightly below the setpoint and the overshoot peak of the subsequent cycle would have the highest possible value of $1+(S_p-1)\times GR$ where GR is the growth ratio for this particular instability. The suppression time delay is smaller than a full oscillation period, which makes the limiting oscillation peak the one occurring in the opposite side of the core a half period later, with an amplitude a factor of \sqrt{GR} greater. Thus the amplitude of a signal at the time of oscillation suppression, S, is obtained in the range

 $1 + (S_p - 1) \times GR^{0.5} < S < 1 + (S_p - 1) \times GR^{1.5}$

The hot channel oscillation magnitude, HCOM, is higher than the OPRM signal magnitude, S, because the latter is a combination of detector responses at several neighboring bundles. However, the maximum signal amplitude and the HCOM are similarly affected by the growth ratio. This explains the need to apply a penalty to the setpoint (or equivalently the HCOM) when an existing HCOM analysis is used for conditions associated with anticipated higher growth ratios compared with the conditions associated with the original analysis.

Following a two-pump-trip, the reactor is brought to natural circulation and power is reduced. The core remains stable until the feedwater heaters respond to the decreased steam flow and the inlet subcooling gradually increases which combined with the resulting power increase bring the core gradually to less stable conditions. The rate of the destabilization depends on the balance of plant (feedwater heaters) not on the operating domain itself. However, operating under extended flow windows (MELLLA+) makes it possible for the final decay ratio to be higher. However, the detection system operates on OPRM signals in the range when coherent signals start (Decay Ratio ≈ 1) to higher growth ratios when the signal amplitude exceeds the relationship between HCOM and the amplitude setpoint as discussed above. It should be noted that the Enhanced Option III solution single channel instability exclusion limits the maximum growth ratio of the signals processed by the detection system. For an exclusion region boundary that crosses the natural circulation line at or below the MELLLA line, no increase in growth ratio is expected and the HCOM versus S_P relationship is not affected by MELLLA+ operation, where the higher growth ratios are anticipated after the operating point crosses into the exclusion region and a scram is initiated.

To put the proposed 5% HCOM penalty in perspective, it is used to allow the use of existing HCOM analysis, while also allowing the possibility to place the exclusion region boundary at or above the MELLLA natural circulation corner. A conservative accounting of the increase in growth ratio is made by biasing the growth ratio probability distribution such that the most likely growth ratio in excess of unity is increased by a factor of ~1.3; in this way for the original probability distribution with a most likely growth ratio of 1.07 the biased distribution would be peaked at a growth ratio of 1.09. Thus biased, the probability of a highly unstable oscillation with a growth ratio of 1.2 is increased by a factor >2 which signifies the high level of conservatism applied due to the probability distribution biasing.

In conclusion, the proposed 5% penalty on existing HCOM versus S_P relationship for application to EO-III is justified as a very conservative approach allowing the single channel instability exclusion region boundary to cross the natural circulation line at or above the MELLLA line. For applications where the single channel instability exclusion region boundary crosses the natural circulation line at a lower power level due to the application of layers of conservatisms in its determination, the 5% HCOM penalty is no longer required.

Question 3: VALIDATION OF THE STEADY-STATE DRYOUT CORRELATIONS

During the ACRS committee presentation, additional data was provided related to the oscillatory flow dryout measurements. Please document this data and provide additional details about the oscillatory dryout benchmarks shown in Section 3.2.3 of BAW-10255(P), including:

- 1. A description of the test conditions for each case,
- 2. A quantitative comparison between predictions of the steady-state dryout correlations and the test data for unstable oscillation conditions,

1

- 3. A statistical evaluation of the errors, and
- 4. An explanation of the temperature drop prior to dryout.

Response 3:

Description of Test Conditions

ANP-10262Q2NP Revision 000 Page 27

Statistical evaluation of the errors:

]

A statistical evaluation of errors is possible for the steady state dryout testing where typically hundreds or thousands of data points are available. [

ANP-10262Q2NP Revision 000 Page 28

]

I

ANP-10262Q2NP Revision 000 Page 29

]

Explanation of the temperature drop prior to dryout:

1

The two-phase flow regime at the plane where dryout is detected is the annular flow regime where a liquid film surrounds the heated rods and the core steam flow carries liquid droplets. The vapor-liquid interface between the film and the core steam is at the saturation condition, while the film-rod interface is superheated where its temperature is higher than the saturation temperature by []. The temperature

gradient across the film drives the heat flux transferring the heat generated in the rods through the liquid film where it is used to provide the energy for evaporating the liquid at the liquid-vapor interface. For a small heated rod control segment at a given elevation, the mass balance of the liquid film is governed by liquid film flow entering and leaving the control segment, the deposition of liquid drops from the core flow and the entrainment of liquid from the film to join the core flow, and the liquid mass loss due to evaporation at the liquid-steam interface.

| | | | | ANP-10262Q2NP | . • |
|-------------------|-----------------------|----------------|---|---------------|-----|
| | ali ka sagara ta si s | | in information in the second secon | Revision 000 | : |
| Response to Reque | st for Additional In | formation – AN | P-10262(P) | Page 30 | |

Additional Discussion

l

The threshold for declaring dryout defined in BAW-10255 was discussed during the ACRS review. This section provides additional background to the issue.

]

1

References

3.1 Reference: Aounallah, Y., "Boiling Suppression in Convective Flow," Proceedings of ICAPP '04, Pittsburgh, PA USA, June 13-17, 2004, Paper 4251.

Example of a turbine flow meter measurement versus pressure drop for growing oscillations [Figure 3-1]

|--|

Figure 3-2 [

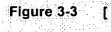
AREVA NP Inc.

ANP-1026202NP

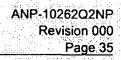
]

Response to Request for Additional Information - ANP-10262(P)

Revision 000 Page 34



AREVA NP Inc.



Ĵ

AREVA NP Inc.

Figure 3-4

I

Question 4: JUSTIFICATION FOR THE 10 PERCENT DIVOM PENALTY FOR MELLLA+

Based on the RAMONA5-FA benchmarks against Karlstein Thermal Hydraulic (KATHY) loop and reactor data and benchmarks of other RAMONA versions, provide a justification why a 10 percent Delta CPR over Initial CPR Versus Oscillation Magnitude (DIVOM curve), penalty bounds any possible RAMONA5-FA uncertainties that may be uncovered by a thorough review of the code. Provide an estimate of the channel decay ratio error that would be required to make the 10 percent DIVOM penalty non-conservative.

The 10 percent DIVOM penalty will likely be applied to the PBDA setpoint calculation; however, it has an equivalent value in terms of an operating limit minimum critical power ratio (OLMCPR) penalty. Assume that the PBDA setpoint remains unchanged (for example at 1.10), and calculate what would be the required increase in OLMCPR to prevent CPR violation during a limiting oscillation that scrams at the constant setpoint, if the DIVOM slope is 10 percent higher. This is the equivalent "CPR penalty" of the 10 percent DIVOM penalty.

Response 4:

Integral benchmarking of RAMONA5-FA with reactor data is dependent on all of the code's models. Benchmarking against KATHY data involves the hydraulics subset of the code's models. Good performance of the code on both sets of benchmarks provides assurance that the good agreement between code results and reactor data is not an artifact of compensating errors between the different code modules.

It must be noted that a DIVOM calculation is essentially an open-loop process while a decay ratio calculation is a closed-loop process. This point can be clarified by briefly describing a density wave oscillation starting from an initial perturbation going through the different models and their effect on DIVOM and decay ratio calculations and applicable experimental data.

An inlet flow rate sinusoidal perturbation travels up the boiling channel. In the non-boiling bottom part of the channel, the magnitude of the flow perturbation is approximately unchanged. As the flow perturbation travels further up the channel, a significant attenuation in the flow rate perturbation occurs and reaches a minimum value at an elevation past the mid-channel height. Past this point, the magnitude of the flow perturbation increases with height until the end of the heated length, but its magnitude normally remains below its value at the channel inlet. A corresponding steam quality perturbation profile is generated, where zero quality perturbation occurs in the non-boiling bottom section, followed by a large increase of the quality perturbation

in the subcooled boiling region, and for higher elevations the magnitude of the quality perturbation continues to decay all the way to the end of the heated length. This density wave profile expressed in flow and quality perturbation magnitudes along the heated length depends on the oscillation frequency. Numerical calculations of the flow and quality profiles depend on solving the continuity equations, provided an inlet perturbation is given in terms of magnitude and frequency. This portion of the density wave is purely kinematic and the fidelity of its modeling in RAMONA5-FA [].

The measured oscillating inlet flow has been used as an input to the code and the resulting calculated quality is used to compute CPR using a well established correlation. The excellent agreement of the calculated CPR response when it approaches unity coinciding with the measured rod temperature spike indicating dryout lead to the conclusion that RAMONA5-FA numerics do not distort the density wave profile.

Furthermore, the quality and flow rate profiles result in a corresponding density (or equivalently void fraction) profile which can be calculated using a void-quality correlation. The integrated density for the entire heated length results in a corresponding pressure drop response which drives the oscillation dynamics. The net effect of the different pressure drop components may lead to an amplified or damped response and determines the frequency of the least stable mode. It is important to recall that the oscillation as represented by the numerical solution of the momentum equation indirectly influence the fidelity of the perturbation profile calculation where an underestimated frequency results in overestimated quality response and vice versa. In this respect, [

shown in Figure 5-2 of BAW-10255 provides assurance that the momentum equation numerical representation in RAMONA5-FA produces the correct frequencies needed for proper calculation of the perturbation profiles. The good agreement obtained for the same tests with regard to hydraulic decay ratios (Figure 5-1 of BAW-10255) is an additional assurance that the void fraction response responsible for the driving density head perturbation is also correct.

Given that exact experimental verification of the RAMONA5-FA quality perturbation profile is not possible, it must be added that the effect of an underestimated quality perturbation will underestimate the CPR response while also underestimating the void response which in turn

underestimating the reactivity and power responses, and vice versa. With both CPR and power responses affected in the same direction, the DIVOM slope remains nearly invariant.

The void fraction plays two main roles in density wave oscillation in a BWR, first through its corresponding density head driving the density wave, and second through the resulting reactivity feedback. With the void fraction response presumed to be correct based on the KATHY tests, the neutron kinetics and pin heat conduction models in RAMONA5-FA are validated by the good agreement with reactor decay ratio and frequency measurements.

Given the unique testing experience behind RAMONA5-FA qualification, and the fact that it has been thoroughly reviewed per AREVA quality assurance requirements, no DIVOM biases are expected. However, it is conceivable that another hypothetical code not so thoroughly qualified may harbor biases.

It is not possible to relate a potential bias in DIVOM slope with a corresponding bias in channel decay ratio without a deeper look at the underlying fundamental cause(s). Generally, as has been demonstrated in Figure 3-2 of ANP-10262, the channel decay ratio variation [

] while producing a (small) DIVOM slope change in opposite directions as shown in Table 6-1 of BAW-10255.

As an engineering judgment, it can be concluded that any DIVOM bias is much smaller than a corresponding decay ratio bias that may result from a code deficiency. The DIVOM variables (relative CPR and power responses) are affected differently but generally in the same direction by altered system responses, which minimizes the impact on the DIVOM slope, while the corresponding decay ratio shift can be large. Given the generic decay ratio uncertainty of nearly

[] commonly associated with code results, the corresponding DIVOM uncertainty should be much less than 10%. In support of this conclusion, attention is brought to the fact that the originally approved generic DIVOM slope was found in good agreement with other calculations including RAMONA5-FA and other codes which are not under review such as RAMONA3. This conclusion applies to extended flow window operation such as MELLLA+ as the core operating

points used for DIVOM calculation in the context of Enhanced Option III resemble current operating conditions at natural circulation.

Equivalent OLMCPR Penalty

An example is presented here for a case with amplitude setpoint $S_{\mu} = 1.1$, for which the Monte Carlo hot channel oscillation magnitude is assumed to be HCOM = (P - M)/A = 0.35. The slope of the DIVOM curve is assumed to be equal to the original generic value of S = 0.45. The safety limit is assumed to be SLMCPR = 1.09.

For a reactor operating at rated conditions at the operating limit, OLMCPR, prior to pump trip, the initial (pre-oscillation), IMCPR, at natural circulation is larger than the operating limit by a factor, R > 1. Thus, $IMCPR = R \times OLMCPR$.

For an oscillation to be successfully suppressed without violation of the safety limit, the operating limit must be equal or larger than the value obtained from the following equation.

$$SLMCPR = R \times OLMCPR \times (1 - S \times HCOM)$$

Neglecting the CPR improvement factor by setting R = 1, and substituting the numerical values of the other parameter as stated above, the operating limit is calculated as

$$OLMCPR = \frac{SLMCPR}{R \times (1 - S \times HCOM)} = \frac{1.09}{1 \times (1 - 0.45 \times 0.35)} = 1.2938$$

When a 10% penalty is applied to the DIVOM slope, the penalty slope becomes $S^* = 0.45 \times 1.1 = 0.495$ which is used to calculate the operating limit with penalty as

$$OLMCPR' = \frac{SLMCPR}{R \times (1 - S' \times HCOM)} = \frac{1.09}{1 \times (1 - 0.495 \times 0.35)} = 1.3184$$

The difference in the OLMCPR is thus 0.025 which is a significant penalty.